

Cite this: *Chem. Commun.*, 2017, 53, 11126Received 18th April 2017,
Accepted 27th June 2017

DOI: 10.1039/c7cc02989f

rsc.li/chemcomm

Turning on the red phosphorescence of a [Ru(tpy)(bpy)(Cl)]Cl complex by amide substitution: self-aggregation, toxicity, and cellular localization of an emissive ruthenium-based amphiphile†

B. Siewert,^{ib}ab M. Langerman,^a Y. Hontani,^c J. T. M. Kennis,^c V. H. S. van Rixel,^a B. Limburg,^a M. A. Siegler,^d V. Talens Saez,^a R. E. Kietlyka,^{ib}a and S. Bonnet^{ib}*a

Coupling the notoriously non-emissive complex [Ru(tpy)(bpy)Cl]Cl (tpy = 2,2':6',2''-terpyridine, bpy = 2,2'-bipyridine) to a C₁₂ alkyl chain via an amide linker on the 4' position of the terpyridine yielded a new amphiphilic ruthenium complex showing red emission and chloride-dependent aggregation properties. This emissive complex is highly cytotoxic in A549 non-small lung cancer cells where it can be followed by confocal microscopy. Uptake occurs within minutes, first by insertion into the cellular membrane, and then by migration to the peri-nuclear region.

Over 80 years ago Francis Burstall reported a reaction between RuCl₃ and 2,2' bipyridine at 250 °C yielding the red salt [Ru(bpy)₃]Cl₂ ([1]Cl₂).¹ The stability of this complex, coupled to its unique electrochemical and photophysical properties, has led to the development of a wide class of octahedral ruthenium polypyridyl complexes² and countless reports on their catalytic,^{2c,3} photosensitizing,⁴ or biological applications.⁵ Depending on the energy level of their triplet excited states, these complexes may be phosphorescent or not. Generally, complexes with three 2,2'-bipyridine (bpy) ligands, e.g. [Ru(bpy)₃]Cl₂ ([1]Cl₂), show a strong emission,^{2a} while complexes containing tridentate 2,2':6',2''-terpyridine ligands (tpy), e.g. [Ru(tpy)₂]Cl₂ ([2]Cl₂), show no emission at room temperature. Negligible phosphorescence was observed for complexes containing both a tpy and a bpy ligand, e.g. [Ru(tpy)(bpy)Cl]Cl ([3]Cl).^{2a,c,6} Emission in [1]²⁺ is due to the high energy gap between the triplet metal-centred (³MC) and triplet metal-to-ligand charge transfer

(³MLCT) excited states (+42.7 kJ mol⁻¹).⁷ In tpy-containing complexes [2]²⁺ and [3]⁺ this ³MC-³MLCT energy gap decreases to -16.7 kJ mol⁻¹⁸ and -6.6 kJ mol⁻¹, respectively,⁹ which promotes non-radiative decay via the ³MC states (Fig. 1). Thermal promotion of the ³MC state from the photochemically generated ³MLCT state may also lead to ligand photosubstitution, in particular for [Ru(tpy)(bpy)(L)]²⁺ complexes (L is a monodentate ligand),^{5e,10} which generates in water the aqua complex [Ru(tpy)(bpy)(OH₂)]²⁺ ([6]²⁺).

When generated in a cell, aqua complexes such as [6]²⁺ may react with biological nucleophiles such as amino acids, peptides (e.g. glutathione), protein residues, or DNA base pairs,¹¹ which – as studied for cisplatin – may lead to cell death. Thus, light-sensitive complexes of the [Ru(tpy)(bpy)(L)]²⁺ type represent an interesting class of pro-drugs: triggering the formation of the active species [6]²⁺ by an external, human-controlled process (i.e. light irradiation), allows for selective drug activation in illuminated tumour tissue, a concept known as photo-activated anticancer

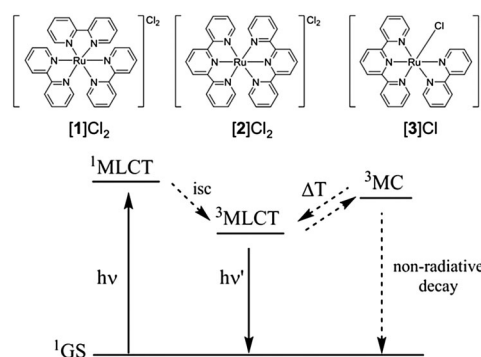


Fig. 1 Top: Chemical structures of [Ru(bpy)₃]Cl₂ ([1]Cl₂), [Ru(tpy)₂]Cl₂ ([2]Cl₂), and [Ru(tpy)(bpy)Cl]Cl ([3]Cl). Bottom: Simplified Jablonski diagram of Ru^{II} polypyridine complexes. The $\Delta E(^3\text{MC}-^3\text{MLCT})$ decreases from [1]²⁺ > [2]²⁺ \approx [Ru(tpy)(bpy)L]²⁺, favouring non-radiative decay for terpyridine-containing complexes via thermally driven population of the ³MC state from the photochemically generated ³MLCT state. (GS = ground state, MLCT = metal-to-ligand charge transfer, isc = intersystem crossing, MC = metal-centred.)

^a Leiden Institute of Chemistry, Leiden University, Einsteinweg 55, 233CC Leiden, The Netherlands. E-mail: bonnet@chem.leidenuniv.nl

^b Institute of Pharmacy, Pharmacognosy, University of Innsbruck, CCB, Innrain 80-82, 6020 Innsbruck, Austria

^c Department of Physics and Astronomy, Vrije Universiteit, De Boelelaan 1081, 1081HV Amsterdam, The Netherlands

^d Small Molecule X-ray Facility, Department of Chemistry Johns Hopkins University, Baltimore, MD 21218, USA

† Electronic supplementary information (ESI) available: Experimental details, Graphical results, and videos. CCDC 1534260. For ESI and crystallographic data in CIF or other electronic format see DOI: 10.1039/c7cc02989f



chemotherapy (PACT).^{12,13} However, as discussed by Alessio,¹⁴ low cellular uptake is an obstacle for charged ruthenium complexes. If the pro-drug does not reach the nucleus, how could lethal metal-DNA adducts be formed? We recently reported that increasing the lipophilicity of a $[\text{Ru}(\text{tpy})(\text{bpy})(\text{L})]^{2+}$ complex by using a cholesterol-thioether ligand L led to a significant increase in cellular uptake, self-aggregating properties, and dark cytotoxicity.^{12a} However, a long pre-irradiation incubation time of 24 h was necessary to observe any phototoxicity, and prodrug localization was impossible to probe *in vitro* because of the non-luminescent character of the ruthenium compound. Here, inspired by Heinze *et al.*¹⁵ we increased the lipophilicity of [3]Cl by conjugating a C₁₂ alkyl tail in 4' position of the tpy ligand *via* an amide linker, and studied whether such mildly electron-withdrawing groups would lead to increased phosphorescence. This communication reports on the synthesis of the amphiphilic complex $[\text{Ru}(\text{Rtpy})(\text{bpy})\text{Cl}]\text{Cl}$ ([4]Cl, Fig. 2, Rtpy = *N*-dodecyl-[2,2':6',2''-terpyridine]-4'-carboxamide), its aggregation properties in aqueous solution, and its significantly improved phosphorescence, which allows for following uptake and localization *in vitro*.

Complex [4]Cl was synthesized in three steps by amide coupling of dodecylamine and 4'-carboxy-2,2':6',2''-terpyridine, followed by coordination to ruthenium trichloride and 2,2'-bipyridine coordination in reductive conditions (Fig. S1, ESI[†]). ¹H NMR experiments disclosed the typical downfield shift of the bpy proton A6, as well as the upfield shift of the B6 proton due to the shielding cone of the tpy ligand. Furthermore, the 3' proton on the amide-functionalized tpy appeared downfield-shifted (9.21 ppm in d₆-DMSO, Fig. S3, ESI[†]) compared to the non-substituted complex [3]⁺ (8.81 ppm, d₆-DMSO). The doubled triplet at 3.46 ppm (³*J* = 6.7 Hz, ³*J* = 6.5 Hz) was assigned to the alpha methylene group of the aliphatic chain due to its coupling with the amide proton. A crystal structure of [4]Cl·H₂O·C₃H₆O was obtained revealing, next to the typical octahedral environment of the ruthenium complexes, a

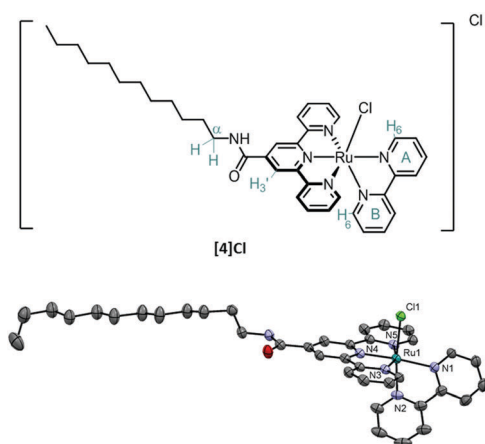


Fig. 2 Top: Chemical formula of complex [4]Cl, and proton numbering scheme for ¹H NMR attribution. Bottom: Displacement ellipsoid plot (50% probability level) of cationic [4]⁺ as observed in the crystal structure of [4]Cl·H₂O·C₃H₆O at 110(2) K. The counter-anion and lattice solvent molecules have been omitted for clarity. Characteristic bond lengths [Å]: Ru1–N1 = 2.077(3), Ru1–N2 = 2.049(3), Ru1–N3 = 2.066(3), Ru1–N4 = 1.954(3), Ru1–N5 = 2.076(3), Ru1–Cl = 2.3956(8).

trans-conformation for the amide bond (Fig. 2 and Fig. S4, ESI[†]), and hydrogen bonding between the chloride counter anion, the water solvate molecule, and the amide group. Finally elemental analysis confirmed the chemical purity of the bulk compound.

In spite of its long alkyl tail [4]Cl was found soluble in aqueous solutions. In water, its UV-vis spectrum (Fig. 3) showed a broad ¹MLCT transition ($d\pi \rightarrow \pi^*$, see HOMO and LUMO in Fig. S20, ESI[†]) with an absorbance maximum bathochromically shifted (502 nm) compared to [3]Cl (484 nm).¹⁶

Remarkably, [4]Cl was also emissive (Fig. 3). In MilliQ water and under air its emission spectrum showed a maximum at 791 nm with an emission quantum yield in air of $\phi_{\text{phos}} = 0.0004$. This quantum yield is two orders of magnitude lower as compared to the reference compound [1]Cl₂ ($\lambda_{\text{max,em}} = 629$ nm, $\phi_{\text{phos,ref}} = 0.04$),¹⁷ but it is still much higher than for [3]Cl, for which quantum yield measurements were impossible.^{2a} The emission intensity increased proportionally to the concentration until 60 μM , indicating no self-quenching in this concentration range (Fig. S7, ESI[†]).¹⁸ Furthermore, the emission spectra in acetonitrile, methanol, or pentane, proved that the emission of [4]Cl in water was not caused by aggregation. The observation of red-shifted emission for [4]Cl compared to [3]Cl indicates that the ³MLCT band lies at significantly lower energy than the ³MC band, which also explains the increased phosphorescence quantum yield: the ³MC–³MLCT gap is higher in [4]⁺ than in [3]⁺, leading to less phosphorescence quenching. Transient absorption spectroscopy (TAS) and time-correlated single photon counting (TCSPC) experiments were done in PBS under air at 7.5 μM and 75 μM , respectively, to investigate the excited state lifetimes of [4]Cl. In PBS, the high chloride concentration prevented formation of the aqua complex $[\text{Ru}(\text{Rtpy})(\text{bpy})(\text{OH}_2)]^{2+}$ ([7]²⁺, see Fig. S9, ESI[†]) that, when formed in pure water, was also emissive (Fig. S8, ESI[†]). Global analysis of the TCSPC data (see Fig. S11 and Table S4, ESI[†]) indicated that the decay of emission of [4]Cl in PBS can be best described by three lifetimes, *i.e.* $\tau_3 = 0.44$ ns (44%), $\tau_{4a} = 9$ ns (14%), and $\tau_{4b} = 40$ ns (42%). TAS (see Fig. S10, ESI[†]), which investigated photon absorption, revealed next to two emission-relevant lifetimes (*i.e.* $\tau_3 = 110$ ps, $\tau_4 = 17$ ns) three lifetimes of non-emissive components (*i.e.* $\tau_1 < 50$ fs, $\tau_2 \sim 3$ ps, and $\tau_5 = 200$ ns). The ultrafast lifetime (*i.e.* $\tau_1 < 50$ fs) might correspond to the intersystem crossing ¹MLCT \rightarrow ³MLCT, which is known to lie

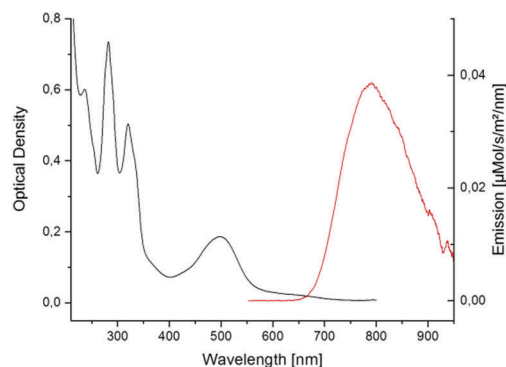


Fig. 3 Absorption and emission spectra of [4]⁺ in MilliQ water and under air. Excitation wavelength was 455 nm (power 50 mW).



in the fs range for ruthenium polypyridyl complexes.¹⁹ The second lifetime ($\tau_2 \sim 3$ ps) was assigned to the vibrational cooling of the ³MLCT(tpy) state, accordingly to reported values.^{10c} The longest component ($\tau_5 = 200$ ns) can be assigned to the non-radiative decay from the excited ³MC states to the GS. The shorter of the two emissive components, *i.e.* $\tau_3 = 110$ ps, showed a slight blue shift and can be correlated to the 0.44 ns component found in TCSPC. Most likely, this lifetime belongs to interconversion (IC) between the ³MC and ³MLCT excited states. The main decay found in TAS, *i.e.* $\tau_4 = 17$ ns, equals the radiative decay from the ³MLCT excited state to the ground state, and was more resolved in TCSPC, where it split into a major (*i.e.* $\tau_{4b} = 40$ ns (42%)) and a minor (*i.e.* $\tau_{4a} = 9$ ns (14%)) component, reflecting the several possible emissive ³MLCT states of ruthenium polypyridyl complexes.²⁰ A schematic overview of the excited state interconversion for compound [4]Cl in PBS is given in Fig. S12, ESI†

In order to investigate the non-radiative decay originating from the ³MC excited states, green light irradiation (490 nm) in water was followed by UV-vis spectroscopy (Fig. S13, ESI†). The kinetics of chloride substitution in [4]⁺ by water, to form the aqua species [Ru(Rtpy)(bpy)(OH₂)]²⁺ ([7]²⁺), was compared with dark conditions. In the dark, thermal hydrolysis was slow, characterized by a hydrolysis rate constant of $k_{\text{hydro}}^{\text{dark}} = 7 \times 10^{-5} \text{ s}^{-1}$. Under green light irradiation the rate constant was enhanced by a factor 24 to $k_{\text{hydro}}^{\text{490nm}} = 2 \times 10^{-3} \text{ s}^{-1}$, corresponding to a photosubstitution quantum yield of 0.0176 (see ESI† part 2.4, Fig. S14). The acceleration of hydrolysis under light irradiation confirmed the TAS results, and indicated that for [4]⁺ the ³MC excited states are thermally accessible, at room temperature, from the photogenerated ³MLCT states.

Further, it was anticipated that the attachment of a long alkyl tail to the 4'-position on the tpy ligand of [4]⁺ may lead to self-assembly.³¹ The morphology of a self-assembled structure can be predicted by calculating the packing parameter P of the surfactant defined as $\nu/(l \cdot a)$, where ν is the volume (in Å³) and l the length (in Å) of the aliphatic chain, while a represents the area of the head group (in Å²).²¹ Employing this equation with values calculated as described in Section 3 of the ESI† the packing parameter P was 0.2. Therewith the assembly of [4]⁺ as spherical micelles is predicted,²² which was studied by DLS and microscopy. Self-assembly of [4]Cl in aqueous solutions was found to highly depend on chloride concentration. Dynamic light scattering (DLS) measurements of [4]Cl in PBS (200 μM) displayed a highly disperse collection of aggregate sizes ranging from a few nanometers to microns in hydrodynamic diameter (d_{H} , see Fig. S16, ESI†). These observations were corroborated by confocal microscopy at a lower concentration (5 μM), which showed the formation of micron-sized, phosphorescent aggregates of micelles (Fig. 4). Zeta potential measurements suggested the formation of charged assemblies ($\zeta = +19.03 \pm 11.1$ mV). In contrast, dissolution of [4]Cl (200 μM) in MilliQ water showed only a single population of stable micelles with a hydrodynamic radius d_{H} of 45 nm, as measured by DLS and further supported by cryo-TEM (Fig. S17, ESI†). Zeta potential measurements showed a 37% increase in charge to $\zeta = +26.1 \pm 7.3$ mV. This increased ζ value may be rationalized by the hydrolysis of

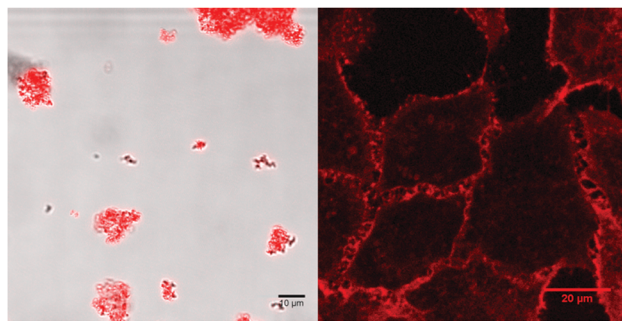


Fig. 4 Left: Confocal fluorescent micrograph of [4]Cl in PBS (5 μM) in absence of fetal bovine serum (FBS) showing micellar aggregation. Right: Confocal fluorescent micrograph of A549 cells incubated with [4]Cl (5 μM) for 15 minutes.

the Ru-Cl bond of [4]⁺ in pure water to form the bicationic aqua complex [7]²⁺, increasing stability of the micellar structure, however the effects of buffer salts on the measured values cannot be excluded (Fig. S16, ESI†). Moreover, the lack of secondary aggregation in pure water as opposed to PBS where micron-sized phosphorescent assemblies were observed (Fig. 4), suggested that micelle aggregation in PBS is driven by the high chloride (137 mM) concentration that stabilizes coordination of the chloride ligand to ruthenium. Similar aggregation phenomena have been documented for other metallo-surfactants.²³ In addition, amide bridging by the chloride counter-ions may affect the secondary aggregation process. Overall, these studies reveal that the self-assembly of [4]Cl in aqueous solutions can be modulated by the chloride concentration.

Our group recently demonstrated that non-emissive ruthenium amphiphiles can be highly toxic to cancer cells by destabilizing the cellular membrane.^{12a} The emissive properties of [4]Cl opened a way to visualize this phenomenon. First, the cytotoxicity of [4]Cl was evaluated *in vitro* on non-small lung cancer cell-line (A549). Whereas – in accordance with the literature¹¹ – [3]Cl showed no measurable toxicity even after incubation for 24 h (see ESI† part 4 for details), its amphiphilic analogue [4]Cl showed significant cytotoxicity after only one hour incubation, characterized by an effective concentration (EC_{50,1h}) of 9.8 μM. This cytotoxic activity increased with incubation time, reaching an EC_{50,24h} value of 2.2 μM after 24 h incubation, which was twice lower than that of cisplatin (EC₅₀ = 4.3 μM). As [4]Cl is phosphorescent, the uptake could this time be followed by optical microscopy time-lapse imaging. The complex was taken up exceptionally quickly, *i.e.* after only a few minutes of incubation (Fig. 4). Time-lapse studies (Video S1, ESI†) showed that the cell membrane was initially stained, as expected due to the amphiphilic character of [4]Cl (Fig. 4). However, it also later internalized: after 9 h (Fig. S19, ESI†) bright emission could be detected in the perinuclear region, indicating that the molecule was enriched probably in the endoplasmic reticulum. Interestingly, the nucleus clearly showed no red emission, as observed by z-stacking (Video S2, ESI†), which indicates either that [4]Cl did not enter the nucleus, or that its emission there was quenched. As instead of stained nuclei spherical red organelles were observed after 9 h incubation, we hypothesize that interaction with nuclear DNA is not likely to explain the toxicity of [4]Cl, but



that exosomes, lysosomes, or even mitochondrial membranes, incorporate the amphiphilic complex [4]Cl, and that the cytotoxicity is based on membrane modulation.

In summary, we report here on compound [4]Cl as a new type of amphiphilic phosphorescent [Ru(tpy)(bpy)(Cl)]⁺ analogue. By attaching an amide group R on the 4'-position of the terpyridine ligand, the ³MLCT level was stabilized just enough to switch on red emission without compromising photosubstitution of the monodentate ligand. By attaching a long alkyl tail to the positively charged ruthenium complex, compound [4]Cl was made amphiphilic and self-assembled in aqueous solutions. Because of the thermal hydrolysis of the Ru–Cl bond, self-assembly was found to depend on chloride concentration: nanometer-scale micelles of the aqua complex [7]²⁺ were found in pure water, while micrometer-scale aggregates of [4]⁺ were characterized in PBS. Whereas the reference compound [3]Cl is essentially not cytotoxic, the amphiphilicity of [4]Cl made it more toxic than cisplatin in A549 cancer cells. Most importantly, red emission now allows for probing cell uptake and localization of the complex by optical microscopy, which was impossible with all previously known ruthenium compounds combining a terpyridine and a bipyridine ligand. Although [4]Cl seemed at short incubation times to behave like a simple soap and to attack the cell membrane, longer incubation times revealed a deeper cellular uptake, no red emission in the nucleus, and accumulation of the compound in the membrane-rich, peri-nuclear region (probably the endoplasmic reticulum). Overall, amide functionalization in 4' position on the terpyridine appears as a very efficient manner to turn on the emission of analogues of [3]Cl without switching off photosubstitution properties. By tuning the functional group attached to the amide, it will be possible to modulate not only the lipophilicity of the complex, as achieved here, but also to introduce cancer-targeting groups for example, which will be critical for the development of PACT complexes based on this type of complexes.

The European Research Council is acknowledged for a Starting Grant to S. B. NWO is acknowledged for a VIDI grant to S. B., a VICI grant and a Middelgroot investment grant to J. T. M. K. The COST action CM1105 is acknowledged for stimulating scientific discussions. Prof. E. Bouwman and Dr S. L. Hopkins are kindly acknowledged for support and scientific discussions, Dr A. Boyle for helping with TEM imaging, and D. Saarloos for synthetic work. Prof. B. Koster, Dr R. I. Koning, and Dr T. Sharp are acknowledged for support and access to the cryoTEM facility at the LUMC.

Notes and references

- 1 F. H. Burstall, *J. Chem. Soc.*, 1936, 173–175.
- 2 (a) A. Juris, V. Balzani, F. Barigelletti, S. Campagna, P. Belser and A. Vonzelewsky, *Coord. Chem. Rev.*, 1988, **84**, 85–277; (b) W. W. Brandt, F. P. Dwyer and E. C. Gyarfás, *Chem. Rev.*, 1954, **54**, 959–1017; (c) J. P. Sauvage, J. P. Collin, J. C. Chambron, S. Guillerez, C. Coudret, V. Balzani, F. Barigelletti, L. Decola and L. Flamigni, *Chem. Rev.*, 1994, **94**, 993–1019; (d) S. Campagna, F. Puntoriero, F. Nastasi, G. Bergamini and V. Balzani, in *Photochemistry and Photophysics of Coordination Compounds I*, ed. V. Balzani and S. Campagna, 2007, vol. 280, pp. 117–214.
- 3 (a) M. Orlandi, R. Argazzi, A. Sartorel, M. Carraro, G. Scorrano, M. Bonchio and F. Scandola, *Chem. Commun.*, 2010, **46**, 3152–3154; (b) H.-W. Tseng, R. Zong, J. T. Muckerman and R. Thummel, *Inorg. Chem.*, 2008, **47**, 11763–11773.
- 4 V. Balzani, A. Juris, M. Venturi, S. Campagna and S. Serroni, *Chem. Rev.*, 1996, **96**, 759–833.
- 5 (a) W. D. Cao, J. P. Ferrance, J. Demas and J. P. Landers, *J. Am. Chem. Soc.*, 2006, **128**, 7572–7578; (b) M. R. Gill, D. Cecchin, M. G. Walker, R. S. Mulla, G. Battaglia, C. Smythe and J. A. Thomas, *Chem. Sci.*, 2013, **4**, 4512–4519; (c) T. Joshi, V. Pierroz, S. Ferrari and G. Gasser, *ChemMedChem*, 2014, **9**, 1419–1427; (d) L. Xu, N.-J. Zhong, H.-L. Huang, Z.-H. Liang, Z.-Z. Li and Y.-J. Liu, *Nucleosides, Nucleotides Nucleic Acids*, 2012, **31**, 575–591; (e) L. M. Loftus, J. K. White, B. A. Albani, L. Kohler, J. J. Kodanko, R. P. Thummel, K. R. Dunbar and C. Turro, *Chem. – Eur. J.*, 2016, **22**, 3704–3708; (f) G. Shi, S. Monro, R. Hennigar, J. Colpitts, J. Fong, K. Kasimova, H. Yin, R. DeCoste, C. Spencer, L. Chamberlain, A. Mandel, L. Lilje and S. A. McFarland, *Coord. Chem. Rev.*, 2015, **282–283**, 127–138; (g) A. Byrne, C. S. Burke and T. E. Keyes, *Chem. Sci.*, 2016, **7**, 6551–6562; (h) A. Martin, A. Byrne, C. Dolan, R. J. Forster and T. E. Keyes, *Chem. Commun.*, 2015, **51**, 15839–15841.
- 6 A. J. Göttle, F. Alary, M. Boggio-Pasqua, I. M. Dixon, J.-L. Heully, A. Bahreman, S. H. C. Askes and S. Bonnet, *Inorg. Chem.*, 2016, **55**, 4448–4456.
- 7 (a) J. Fan, S. Tysoe, T. C. Streckas, H. D. Gafney, N. Serpone and D. Lawless, *J. Am. Chem. Soc.*, 1994, **116**, 5343–5351; (b) J. Van Houten and R. J. Watts, *J. Am. Chem. Soc.*, 1976, **98**, 4853–4858.
- 8 O. A. Borg, S. S. M. C. Godinho, M. J. Lundqvist, S. Lunell and P. Persson, *J. Phys. Chem. A*, 2008, **112**, 4470–4476.
- 9 E. Jakubikova, W. Chen, D. M. Dattelbaum, F. N. Rein, R. C. Rocha, R. L. Martin and E. R. Batista, *Inorg. Chem.*, 2009, **48**, 10720–10725.
- 10 (a) J. D. Knoll, B. A. Albani and C. Turro, *Chem. Commun.*, 2015, **51**, 8777–8780; (b) R. E. Goldbach, I. Rodriguez-Garcia, J. H. van Lenthe, M. A. Siegler and S. Bonnet, *Chem. – Eur. J.*, 2011, **17**, 9924–9929; (c) J. D. Knoll, B. A. Albani and C. Turro, *Acc. Chem. Res.*, 2015, **48**, 2280–2287.
- 11 O. Novakova, J. Kasparkova, O. Vrana, P. M. van Vliet, J. Reedijk and V. Brabec, *Biochemistry*, 1995, **34**, 12369–12378.
- 12 (a) B. Siewert, V. H. S. van Rixel, E. J. van Rooden, S. L. Hopkins, M. J. B. Moester, F. Ariese, M. A. Siegler and S. Bonnet, *Chem. – Eur. J.*, 2016, **22**, 10960–10968; (b) L. N. Lameijer, S. L. Hopkins, T. G. Brevé, S. H. C. Askes and S. Bonnet, *Chem. – Eur. J.*, 2016, **22**, 18484–18491.
- 13 (a) C. Mari, V. Pierroz, S. Ferrari and G. Gasser, *Chem. Sci.*, 2015, **6**, 2660–2686; (b) S. Bonnet, *Comments Inorg. Chem.*, 2015, **35**, 179–213.
- 14 E. Alessio, *Eur. J. Inorg. Chem.*, 2016, 1549–1560.
- 15 (a) K. Heinze, K. Hempel and M. Beckmann, *Eur. J. Inorg. Chem.*, 2006, 2040–2050; (b) J. Dietrich, U. Thorenz, C. Förster and K. Heinze, *Inorg. Chem.*, 2013, **52**, 1248–1264; (c) A. Breivogel, M. Meister, C. Förster, F. Laquai and K. Heinze, *Chem. – Eur. J.*, 2013, **19**, 13745–13760; (d) A. Breivogel, C. Kreitner and K. Heinze, *Eur. J. Inorg. Chem.*, 2014, 5468–5490.
- 16 M. Maestri, N. Armaroli, V. Balzani, E. C. Constable and A. Thompson, *Inorg. Chem.*, 1995, **34**, 2759–2767.
- 17 K. Suzuki, A. Kobayashi, S. Kaneko, K. Takehira, T. Yoshihara, H. Ishida, Y. Shiina, S. Oishi and S. Tobita, *Phys. Chem. Chem. Phys.*, 2009, **11**, 9850–9860.
- 18 (a) A. Aliprandi, M. Mauro and L. De Cola, *Nat. Chem.*, 2016, **8**, 10–15; (b) M. Mauro, G. De Paoli, M. Otter, D. Donghi, G. D'Alfonso and L. De Cola, *Dalton Trans.*, 2011, **40**, 12106–12116.
- 19 S. Yoon, P. Kukura, C. M. Stuart and R. A. Mathies, *Mol. Phys.*, 2006, **104**, 1275–1282.
- 20 F. Alary, J. L. Heully, L. Bijeire and P. Vicendo, *Inorg. Chem.*, 2007, **46**, 3154–3165.
- 21 J. N. Israelachvili, D. J. Mitchell and B. W. Ninham, *J. Chem. Soc., Faraday Trans.*, 1976, **72**, 1525–1568.
- 22 R. Nagarajan, *Langmuir*, 2002, **18**, 31–38.
- 23 (a) T. A. Wagay, J. Dey, S. Kumar, V. K. Aswal and K. Ismail, *RSC Adv.*, 2016, **6**, 66900–66910; (b) T. A. Wagay, J. Dey, S. Kumar, V. K. Aswal and K. Ismail, *Colloids Surf., A*, 2016, **503**, 61–69.

